

Vortex end Majorana zero modes in superconducting Dirac and Weyl semimetals

Zhongbo Yan,^{1,*} Zhigang Wu,^{2,3} and Wen Huang²

¹*School of Physics, Sun Yat-Sen University, Guangzhou 510275, China*

²*Guangdong Provincial Key Laboratory of Quantum Science and Engineering,
Shenzhen Institute for Quantum Science and Engineering,*

Southern University of Science and Technology, Shenzhen 518055, Guangdong, China

³*Center for Quantum Computing, Peng Cheng Laboratory, Shenzhen 518005, China*

(Dated: August 18, 2024)

Time-reversal invariant (TRI) Dirac and Weyl semimetals in three dimensions (3D) can host open Fermi arcs and spin-momentum locking Fermi loops on the surfaces. We find that when they become superconducting with s -wave pairing and the doping is lower than a critical level, straight π -flux vortex lines terminating at surfaces with Fermi arcs or spin-momentum locking Fermi loops can realize 1D topological superconductivity and harbor Majorana zero modes at their ends. Remarkably, we find that the vortex-generation-associated Zeeman field can open (when the surfaces have only Fermi arcs) or enhance the topological gap protecting Majorana zero modes, which is contrary to the situation in superconducting topological insulators. By studying the tilting effect of bulk Dirac and Weyl cones, we further find that type-I Dirac and Weyl semimetals in general have a much broader topological regime than type-II ones. Our findings build up a connection between TRI Dirac and Weyl semimetals and Majorana zero modes in vortices.

Majorana zero modes (MZMs) localised in the vortices of the superconducting order parameter have been actively sought after for more than a decade[1–8]. Originally, they were predicted to exist in 2D chiral p -wave superconductors[9], but the scarcity of such superconductors in nature compels the community to look for other possible candidates. A breakthrough comes with the realization that when the spin-momentum locking Dirac surface states of 3D topological insulators (TIs) are gapped by s -wave superconductivity, a π -flux vortex carries a single MZM at its core[10]. Since then, TIs with either proximity-induced or intrinsic superconductivity are strongly desired for the realization of MZMs in experiment[11–20]. Remarkably, the normal state of several iron-based superconductors has recently been found to carry an inverted band structure and thus Dirac surface states[21–23]. In superconducting states, zero-bias peaks, as well as several other ordered discrete peaks, are clearly observed in scanning tunnelling spectroscopy of these materials when the tip moves close to the vortex core[24–30], thus providing strong experimental evidences for the existence of MZMs in the vortices of these superconductors.

In efforts to broaden the scope of materials that can host MZMs in vortices, the question of whether the bulk material needs to be insulating has been naturally raised[31–36]. The finding that the MZMs survive even in the doped TI with metallic normal states[31] has motivated us to examine the possibility of MZMs appearing in the recently discovered 3D Dirac and Weyl semimetals[37–49], though their bulk and boundary physics display remarkable difference compared with TIs[50, 51]. With respect to the bulk, the energy bands of Dirac and Weyl semimetals touch at some isolated points (the so-called Dirac and Weyl points) away from which the dispersions are distinct from those of conventional quasiparticles in metals and are responsible for some novel transport properties[52–54]. On the boundary, a hallmark is the existence of open Fermi arcs which connect the projections of the

bulk Dirac and Weyl points[47, 48]. Such Fermi arcs have attracted great research interest as they can result in many remarkable phenomena[55–58].

Intriguingly, when time-reversal symmetry is preserved, spin-momentum locking Fermi loops (abbreviated as “Fermi loops” below), a manifestation of Dirac surface states, can co-exist with the Fermi arcs on the surfaces of Dirac and Weyl semimetals[59–62]. With this observation and the scenario in doped TIs in mind, we study π -flux vortex lines terminating at such surfaces and do find the existence of MZMs at the vortex ends below a critical doping level. Strikingly, we find that the topological gap of the vortex line protecting MZMs in superconducting Dirac and Weyl semimetals can be profoundly enhanced by the vortex-generation-associated Zeeman field, which is contrary to the situation in superconducting TIs. Importantly, we also find that the Zeeman field can lead to the realization of vortex-end MZMs even when the surfaces have only Fermi arcs, indicating the generality of the underlying physics. In addition, we find that the vortex lines in type-I Dirac and Weyl semimetals have a much broader topological regime than those in the type-II ones.

Fermi arcs and Fermi loops.— We begin with the normal state Hamiltonian, which reads[63]

$$H_0(\mathbf{k}) = \varepsilon(\mathbf{k}) + (m - t \cos k_x - t \cos k_y - t_3 \cos k_z)\sigma_z \\ + t' \sin k_x \sigma_x s_z + t'_3 \sin k_z (\cos k_x - \cos k_y) \sigma_x s_x \\ - t' \sin k_y \sigma_y + 2t'_3 \sin k_z \sin k_x \sin k_y \sigma_x s_y + \delta \sigma_y s_z (1)$$

in the basis $\Psi_{\mathbf{k}}^\dagger = (c_{1,\uparrow,\mathbf{k}}^\dagger, c_{2,\uparrow,\mathbf{k}}^\dagger, c_{1,\downarrow,\mathbf{k}}^\dagger, c_{2,\downarrow,\mathbf{k}}^\dagger)$, where the Pauli matrices σ_i and s_i with $i = \{x, y, z\}$ act in the orbit and spin spaces respectively. For notational simplicity, identity matrices σ_0 and s_0 are made implicit and the lattice constant is set to unit throughout the whole work. $\varepsilon(\mathbf{k})$ is a term characterizing the asymmetry of conduction and valence bands. In this work, we take $\varepsilon(\mathbf{k}) = 0$ for simplicity unless otherwise specified. When $\delta = 0$, $H_0(\mathbf{k})$ has time-reversal symmetry, inversion symmetry and C_{4z} -rotational symme-

try. These symmetries stabilize Dirac points on rotational-symmetry axes. A finite δ breaks the inversion symmetry and consequently splits a Dirac point into two Weyl points with opposite chirality, as illustrated in Fig.1(a).

While the two t'_3 -terms are often ignored in the study of Dirac and Weyl semimetals, they are in fact ubiquitous in real materials as they are allowed by symmetry[59, 61]. Although they do not (or weakly) affect the linear dispersion near the Dirac (or Weyl) points, they do have a strong impact on the boundary modes. To see this, we examine the system occupying the region $0 \leq x \leq L$ (L assumed to be very large) and use the edge theory to obtain the low-energy Hamiltonians describing the boundary modes on the $x = 0$ and $x = L$ surfaces[64]. By considering that the band inversion occurs at the Γ point, we find that they are respectively given by (derivation details are provided in the Supplemental Material (SM)[65])

$$\begin{aligned} H_{S;0}(k_y, k_z) &= -\delta + v_y k_y s_z + v_z(k_y, k_z) k_z s_y, \\ H_{S;L}(k_y, k_z) &= \delta - v_y k_y s_z - v_z(k_y, k_z) k_z s_y, \end{aligned} \quad (2)$$

where $v_y = t'$, $v_z(k_y, k_z) = -t'_3(\tilde{m} + tk_y^2 + t_3k_z^2/2)/t$, $\tilde{m} = m - 2t - t_3$, and the boundary modes exist within the regime $tk_y^2/2 + t_3k_z^2/2 < -\tilde{m}$. In the absence of the t'_3 -terms, i.e., $t'_3 = 0$, it is readily found that $v_z(k_y, k_z) = 0$ and each Hamiltonian in Eq.(2) describes a pair of 1D helical modes reminiscent of 2D TIs. However, once $t'_3 \neq 0$, each Hamiltonian in Eq.(2) describes a 2D Dirac cone at $\bar{\Gamma} = (0, 0)$ in the leading order, which is reminiscent of 3D TIs. Moreover, one can see that the δ term only induces an energy shift of the Dirac cones. The above analyses show that Dirac surface states exist not only in TIs, but also in TRI Dirac and Weyl semimetals.

In Figs.1(b)(c)(d), we present the constant-energy contours of surface states (CECSS) for various choices of t'_3 and δ . According to Eq.(2), the CECSS at energy E_s are determined by $\pm\delta \pm \sqrt{v_y^2 k_y^2 + v_z^2(k_y, k_z) k_z^2} = E_s$ under the constraint $tk_y^2/2 + t_3k_z^2/2 < -\tilde{m}$. Fig.1(b) shows that when $t'_3 = \delta = 0$, the CECSS on the $x = 0$ surface are two open Fermi arcs whose spin textures are opposite due to time-reversal symmetry. It is worth pointing out that for the Dirac semimetal, i.e., $\delta = 0$, Eq.(2) indicates that the CECSS on the $x = 0$ and $x = L$ surface coincide and display opposite spin textures, so we only present the results on the $x = 0$ surface for clarity. Fig.1(c) shows that when $t'_3 \neq 0$, $\delta = 0$, the CECSS on the $x = 0$ surface contains two open Fermi arcs and one Fermi loop. As one Dirac point is equivalent to two Weyl points with opposite chirality, one can see that the open Fermi arcs in Fig.1(c) begin and end at the same projection of bulk Fermi surfaces. When δ becomes nonzero, the CECSS on the $x = 0$ and $x = L$ surfaces no longer coincide. Fig.1(d) shows that while two Fermi arcs and one Fermi loop coexist on the $x = L$ surface, the $x = 0$ surface only contains two Fermi arcs.

Vortex bound states in superconducting Dirac and Weyl semimetals.— Two groups have recently found that a π -flux vortex line parallel to the rotational-symmetry axis in super-

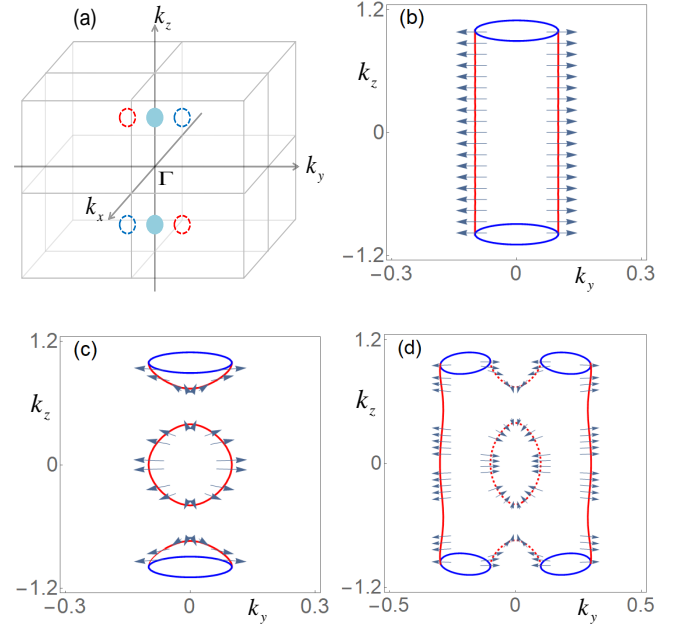


FIG. 1. (a) A schematic diagram of Dirac and Weyl points in Brillouin zone. The filled dots on the k_z axis represent Dirac points. Breaking inversion symmetry splits the two Dirac points into four Weyl points (the four unfilled dots, the red and blue colors represent opposite chirality). In (b)(c)(d), the red lines represent the constant-energy contours of surface states at energy $E_s = 0.1$, the blue lines represent the projection of bulk Fermi surfaces at Fermi energy $E_F = E_s$ in the k_y - k_z plane, and the arrows show the spin textures of the surface states. Common parameters are $m = 2.5$ and $t = t_3 = t' = 1$. (b) $t'_3 = \delta = 0$. Two open Fermi arcs connect the projections of bulk Fermi surfaces tangentially. (c) $t'_3 = 0.6, \delta = 0$. A Fermi loop coexists with two Fermi arcs. (d) $t'_3 = 0.6, \delta = 0.2$. The red solid lines are Fermi arcs on the $x = 0$ surface, and the red dashed lines are Fermi arcs and Fermi loop on the $x = L$ surface.

conducting Dirac semimetals hosts 1D propagating Majorana modes[63, 66]. There the vortex line is terminated at the z -normal surfaces without any Fermi arc or loop. In this work, we consider π -flux vortex lines along the x direction and explore the consequence of Fermi arcs and loops on the x -normal surfaces.

When the TRI Dirac and Weyl semimetals become superconducting and vortex lines are generated along the x direction by an external magnetic field, the system is described by $H = \frac{1}{2} \sum_{\mathbf{r}, \mathbf{r}'} \Psi_{\mathbf{r}}^\dagger H_{\text{BdG}}(\mathbf{r}, \mathbf{r}') \Psi_{\mathbf{r}'}$, with the basis $\Psi_{\mathbf{r}}^\dagger = (c_{1,\uparrow,\mathbf{r}}^\dagger, c_{2,\uparrow,\mathbf{r}}^\dagger, c_{1,\downarrow,\mathbf{r}}^\dagger, c_{2,\downarrow,\mathbf{r}}^\dagger, c_{1,\uparrow,\mathbf{r}}, c_{2,\uparrow,\mathbf{r}}, c_{1,\downarrow,\mathbf{r}}, c_{2,\downarrow,\mathbf{r}})$ and the real-space Bogoliubov-de Gennes (BdG) Hamiltonian

$$H_{\text{BdG}}(\mathbf{r}, \mathbf{r}') = \begin{pmatrix} H_{\mathbf{r},\mathbf{r}'} & \Delta_{\mathbf{r},\mathbf{r}'} \\ \Delta_{\mathbf{r}',\mathbf{r}}^\dagger & -H_{\mathbf{r}',\mathbf{r}}^T \end{pmatrix}, \quad (3)$$

where $H_{\mathbf{r},\mathbf{r}'} = H_{0;\mathbf{r},\mathbf{r}'} + V_{z;\mathbf{r},\mathbf{r}'} - \mu_{\mathbf{r},\mathbf{r}'}$ with $H_{0;\mathbf{r},\mathbf{r}'}$ being the Fourier transformation of $H_0(\mathbf{k})$ in Eq.(1), $V_{z;\mathbf{r},\mathbf{r}'} = \frac{1}{2} g \mu_B B s_x \delta_{\mathbf{r},\mathbf{r}'} \equiv V_z s_x \delta_{\mathbf{r},\mathbf{r}'}$ represents the vortex-generation-associated Zeeman field whose impact depends on both the magnetic field B and the material-dependent g

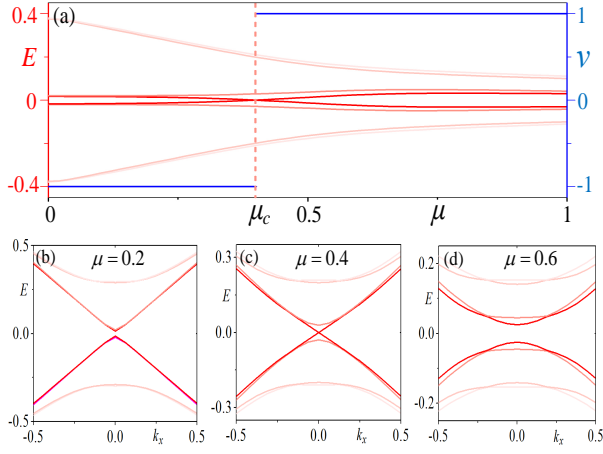


FIG. 2. The evolution of vortex bound states (only the lowest few states are shown) with respect to doping level μ . Common parameters are $m = 2.5$, $t = t_3 = t'_3 = 1$, $V_z = 0$, $\delta = 0$, $\Delta_0 = 0.5$, $\xi = 4$, $L_y = L_z = 20$. (a) Vortex bound states at $k_x = 0$. There is a crossing at $\mu_c = 0.4$, where the Z_2 invariant (blue line) also jumps and indicates that a vortex phase transition takes place. (b)(c)(d) The dispersions of vortex bound states at different values of μ . The bound states at $k_x = \pi$ remains gapped with the increase of μ , while the bound states at $k_x = 0$ undergoes a gap closure at μ_c .

factor[65], and $\mu_{r,r'} = \mu\delta_{r,r'}$ is the chemical potential; $\delta_{r,r'}$ is the Kronecker symbol; $\Delta_{r,r'}$ is the superconducting order parameter. Similarly to Refs.[63, 66], here we consider a spin-singlet s -wave pairing, i.e., $\Delta_{r,r'} = -i\Delta(\mathbf{r})s_y\delta_{r,r'}$, which fully gaps the bulk states when the Zeeman field is smaller than its amplitude. To model a vortex line in the x direction, we assume $\Delta(\mathbf{r}) = \Delta_0 \tanh(\sqrt{y^2 + z^2}/\xi)e^{i\theta}$ where $\theta = \arctan(y/z)$ and ξ is the coherence length. The vortex line breaks the translational symmetry in the yz plane and the time-reversal symmetry, therefore, the 3D superconducting system can be viewed as a 1D superconductor whose unit cell contains all lattice sites in the yz plane. Accordingly, the system belongs to the class D of the Atland-Zirnbauer classification and is characterized by a Z_2 invariant if its energy spectrum is fully-gapped[67, 68]. The Z_2 invariant is given by[65, 69, 70]

$$\nu = \text{sgn}(\text{Pf}(A(k_x = 0))) \cdot \text{sgn}(\text{Pf}(A(k_x = \pi))), \quad (4)$$

where $A(k_x)$ denotes the BdG Hamiltonian in the Majorana representation i.e., $H = i \sum_{k_x} \gamma_{k_x} A(k_x) \gamma_{-k_x}$ with γ_{k_x} denoting the Majorana basis[65], and $\text{Pf}(A(k_x))$ denotes the Pfaffian of the antisymmetric matrix $A(k_x)$. The sign function $\text{sgn}(x) = 1(-1)$ for $x > (<)$ 0. And $\nu = -1/1$ corresponds to a topological/trivial vortex line with/without robust MZMs appearing at its ends.

Let us first focus on the superconducting Dirac semimetal with finite t'_3 terms and ignore the Zeeman splitting. Because the band inversion is considered to occur at the Γ point and the MZMs are related to the low-energy excitations of the normal state, Eq.(4) implies that we can focus on $k_x = 0$ as long as the Fermi level is not doped too far away from the Dirac

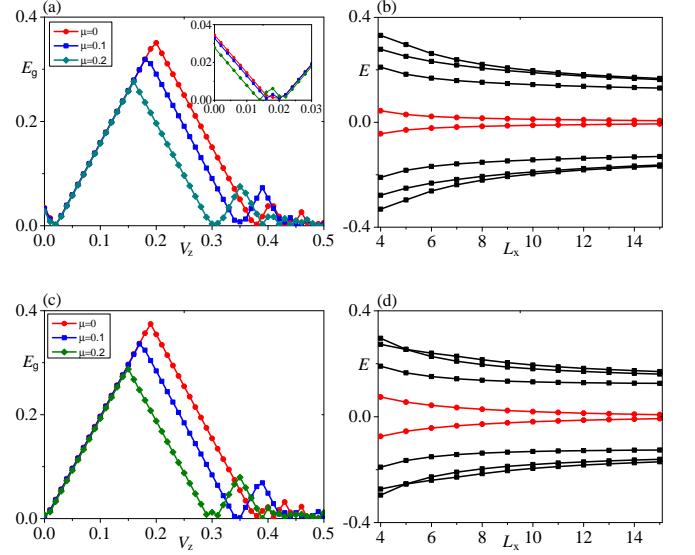


FIG. 3. (a)(c) The evolution of energy gap at $k_x = 0$ with respect to Zeeman field, the inset in (a) is an enlarged view of the low-field regime. (b)(d) The energy spectra for a cubic sample with open boundary condition in all three directions (only the eight energies closest to zero are shown). Common parameters are $m = 2.5$, $t = t_3 = t'_3 = 1$, $\delta = 0$, $\Delta_0 = 0.5$, $\xi = 4$. $L_y = L_z = 20$ in (a)(c), $L_y = L_z = 8$ in (b)(d), $t'_3 = 1$ in (a)(b), $t'_3 = 0$ in (c)(d), $\mu = 0$ and $V_z = 0.2$ in (b)(d).

points. In Fig.2, we present the numerical results of the evolution of the dispersions for vortex bound states and the Z_2 invariant under the variation of μ , i.e., the doping level (only $\mu > 0$ is shown as the result is found to be symmetric about $\mu = 0$). For clarity, we have only shown eight bound states closest to zero energy. The results reveal that the vortex line is full-gapped except at μ_c where a vortex phase transition takes place. Similarly to superconducting TIs[31], we find $\nu = -1$ when the doping is below a critical level, signaling the realization of 1D topological superconductivity on the vortex line. In spite of the similarity in the topological phase diagram, there are profound distinctions between the vortex lines of superconducting Dirac semimetals and those of superconducting TIs. One is that the π -Berry phase developed to explain the vortex phase transition for the latter[31] does not apply to the former[65], owing to their fundamental differences in normal states. Moreover, as will be shown below, the effect of Zeeman field to the vortex lines is completely different for these two classes of systems.

Keeping the finite value of t'_3 , Fig.3(a) shows how the energy gap of the vortex line at $k_x = 0$ (denoted by E_g) evolves with the Zeeman field for $\mu = 0, 0.1, 0.2$. It is readily found that E_g first decreases and gets closed twice at two very small and close V_z (see the inset of Fig.3(a)) and then increases linearly to values much greater than the zero-field value. Here the double closures of E_g are simply because the lowest excitation spectra of the vortex line are nearly doubly degenerate

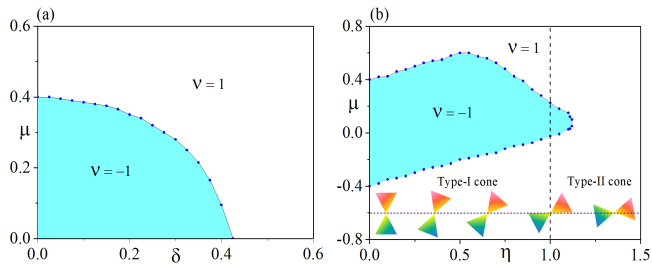


FIG. 4. (a) The topological phase diagram for the superconducting Weyl semimetal. (b) The effect of tilting of Dirac cones, characterized by the η parameter, on the topological regime of the vortex line. Common parameters in (a) and (b) are $m = 2.5$, $t = t_3 = t' = t'_3 = 1$, $\Delta_0 = 0.5$, $\xi = 4$, $L_y = L_z = 20$.

(see Fig.2). Since ν changes its value for each closure and reopening of E_g , ν returns its zero-field value after entering the gap-linear-increase regime. Our numerical calculations of ν confirm the above arguments. This fact reveals that the Zeeman field can greatly enhance the topological gap protecting MZMs in the weakly-doped regime. To further support this, we diagonalize the Hamiltonian for a cubic geometry with open boundary condition in all three directions. In Fig.3(b), we present the eight energies closest to $E = 0$ for $\mu = 0$ and $V_z = 0.2$ ($\nu = -1$ for this case), their scalings with the system size clearly reveal the existence of two MZMs.

Fig.3(c) shows the E_g - V_z dependence in the limit $t'_3 = 0$. In comparison to Fig.3(a), a qualitative difference appears in the low-field regime. In Fig.3(c), the energy gap is vanishingly small at $V_z = 0$, indicating the crucial role of the t'_3 terms in the realization of robust MZMs when the Zeeman field is negligible. Remarkably, away from the low-field regime, Figs.3(c) and (a) show little difference, revealing the important fact that vortex-end MZMs can also be realized in Dirac semimetals with only Fermi arcs (see Fig.3(d)). In sharp contrast, we find that the Zeeman field monotonically reduces the topological gap of the vortex lines in superconducting TIs (see details in SM[65]).

As the stability of MZMs does not need any crystal symmetry, it is obvious that vortex-end MZMs can also be realized when δ is finite but small. In Fig.4(a), we present the impact of δ on μ_c . For simplicity, we only show the result for finite t'_3 and $V_z = 0$ [65]. The phase diagram suggests that increasing δ , which increases the separation between Weyl points, decreases the topological regime but in a considerably smooth way, indicating that vortex-end MZMs can also be realized in many Weyl semimetals when they become superconducting.

The effect of tilting.— Dirac and Weyl semimetals have commonly been divided into two classes, i.e. type-I and type-II [71], in accordance with the extent of tilting of Dirac and Weyl cones. To capture the effect of tilting, here we let the so far ignored $\varepsilon(\mathbf{k})$ term in Hamiltonian (1) take the form $\varepsilon(\mathbf{k}) = \eta t_3 (\cos k_z - \cos k_0)$, where $\pm k_0$ are the coordinates of Dirac or Weyl points in the k_z direction and η characterizes the extent of tilting, with $\eta < 1$ and $\eta > 1$ corresponding

respectively to the type-I and type-II phase.

Since the tilting effects for the Dirac semimetal and the Weyl semimetal are found to share qualitatively the same picture, here we only present the results for the former and present the results for the latter in the SM[65]. As shown in Fig.4(b), the topological regime barely changes for $\eta < 0.5$ but it shrinks as η increases further. After entering into the type-II phase, it is found to vanish quickly, suggesting that type-II Dirac semimetals are less favored than type-I ones for the realization of vortex-end MZMs.

Experimental consideration.— As superconductivity has already been observed in quite a few TRI Dirac and Weyl semimetals [72–88], our predictions are immediately testable in experiment. A very promising class of platforms are semimetal/superconductor hybrid structures, like the experimentally studied $\text{Cd}_3\text{As}_2/\text{Nb}$ [88]. As is known, Cd_3As_2 is an ideal Dirac semimetal with the Fermi energy very close to the two Dirac points[41], therefore, when it becomes superconducting due to the proximity effect of the s -wave superconductor Nb, the vortex lines terminating at the surfaces with Fermi arcs are expected to host MZMs at their ends. Furthermore, Dirac points close to Fermi energy have also been observed in several iron-based superconductors[23], e.g., $\text{FeTe}_x\text{Se}_{1-x}$ and $\text{LiFe}_{1-x}\text{CoAs}$. Our findings can also be tested in these intrinsic superconductors by tuning the doping level to be closer to the Dirac points.

Conclusion.— We have revealed that MZMs can be realized at the ends of a π -flux vortex line in superconducting TRI Dirac and Weyl semimetals if the vortex line is terminated at the surfaces with Fermi arcs or loops and the doping is lower than a critical level, and remarkably, the Zeeman field can profoundly enhance the stability of MZMs in these systems. We have also shown that type-I Dirac and Weyl semimetals are in general more favorable than type-II ones for the realization of MZMs. Our findings offer a new perspective on the potential applications of topological semimetals.

Acknowledgements.— Z.Y. would like to thank the hospitality of Shenzhen Institute for Quantum Science and Engineering at Southern University of Science and Technology and Peng Cheng Laboratory, where this work was started. Z.Y. acknowledges the support by the Startup Grant (No. 74130-18841219) and the National Science Foundation of China (Grant No.11904417). Z.W. acknowledges the support by the National Science Foundation of China (Grant No.11904417) and the Key-Area Research and Development Program of Guangdong Province (Grant No.2019B030330001). W.H. is supported by the National Science Foundation of China (Grant No. 11904155), and by the Guangdong Provincial Key Laboratory (Grant No.2019B121203002).

* yanzhb5@mail.sysu.edu.cn

[1] Jason Alicea, “New directions in the pursuit of majorana fermions in solid state systems,” Reports on Progress in Physics

- 75, 076501 (2012).
- [2] C. W. J. Beenakker, "Search for Majorana Fermions in Superconductors," *Annual Review of Condensed Matter Physics* **4**, 113–136 (2013).
 - [3] Tudor D Stanescu and Sumanta Tewari, "Majorana fermions in semiconductor nanowires: fundamentals, modeling, and experiment," *Journal of Physics: Condensed Matter* **25**, 233201 (2013).
 - [4] Martin Leijnse and Karsten Flensberg, "Introduction to topological superconductivity and majorana fermions," *Semiconductor Science and Technology* **27**, 124003 (2012).
 - [5] Steven R. Elliott and Marcel Franz, "*Colloquium* : Majorana fermions in nuclear, particle, and solid-state physics," *Rev. Mod. Phys.* **87**, 137–163 (2015).
 - [6] Sankar Das Sarma, Michael Freedman, and Chetan Nayak, "Majorana zero modes and topological quantum computation," *npj Quantum Information* **1**, 15001 (2015).
 - [7] Masatoshi Sato and Satoshi Fujimoto, "Majorana fermions and topology in superconductors," *Journal of the Physical Society of Japan* **85**, 072001 (2016).
 - [8] R. Aguado, "Majorana quasiparticles in condensed matter," *ArXiv e-prints* (2017), arXiv:1711.00011 [cond-mat.supr-con].
 - [9] N. Read and Dmitry Green, "Paired states of fermions in two dimensions with breaking of parity and time-reversal symmetries and the fractional quantum hall effect," *Phys. Rev. B* **61**, 10267–10297 (2000).
 - [10] Liang Fu and C. L. Kane, "Superconducting proximity effect and majorana fermions at the surface of a topological insulator," *Phys. Rev. Lett.* **100**, 096407 (2008).
 - [11] Y. S. Hor, A. J. Williams, J. G. Checkelsky, P. Roushan, J. Seo, Q. Xu, H. W. Zandbergen, A. Yazdani, N. P. Ong, and R. J. Cava, "Superconductivity in $\text{Cu}_x\text{Bi}_2\text{Se}_3$ and its implications for pairing in the undoped topological insulator," *Phys. Rev. Lett.* **104**, 057001 (2010).
 - [12] L Andrew Wray, Su-Yang Xu, Yuqi Xia, Yew San Hor, Dong Qian, Alexei V Fedorov, Hsin Lin, Arun Bansil, Robert J Cava, and M Zahid Hasan, "Observation of topological order in a superconducting doped topological insulator," *Nature Physics* **6**, 855 (2010).
 - [13] M. Kriener, Kouji Segawa, Zhi Ren, Satoshi Sasaki, and Yoichi Ando, "Bulk superconducting phase with a full energy gap in the doped topological insulator $\text{Cu}_x\text{Bi}_2\text{Se}_3$," *Phys. Rev. Lett.* **106**, 127004 (2011).
 - [14] Satoshi Sasaki, M. Kriener, Kouji Segawa, Keiji Yada, Yukio Tanaka, Masatoshi Sato, and Yoichi Ando, "Topological superconductivity in $\text{Cu}_x\text{Bi}_2\text{Se}_3$," *Phys. Rev. Lett.* **107**, 217001 (2011).
 - [15] Mei-Xiao Wang, Canhua Liu, Jin-Peng Xu, Fang Yang, Lin Miao, Meng-Yu Yao, CL Gao, Chenyi Shen, Xucun Ma, X Chen, *et al.*, "The coexistence of superconductivity and topological order in the Bi_2Se_3 thin films," *Science* **336**, 52–55 (2012).
 - [16] Eryin Wang, Hao Ding, Alexei V. Fedorov, Wei Yao, Zhi Li, Yan-Feng Lv, Kun Zhao, Li-Guo Zhang, Zhijun Xu, John Schneeloch, Ruidan Zhong, Shuai-Hua Ji, Lili Wang, Ke He, Xucun Ma, Genda Gu, Hong Yao, Qi-Kun Xue, Xi Chen, and Shuyun Zhou, "Fully gapped topological surface states in Bi_2Se_3 films induced by a d-wave high-temperature superconductor," *Nature Physics* **9**, 621 (2013).
 - [17] Parisa Zareapour, Alex Hayat, Shu Yang F. Zhao, Michael Kreshchuk, Achint Jain, Daniel C. Kwok, Nara Lee, Sang-Wook Cheong, Zhijun Xu, Alina Yang, G.D. Gu, Shuang Jia, Robert J. Cava, and Kenneth S. Burch, "Proximity-induced high-temperature superconductivity in the topological insulators Bi_2Se_3 and Bi_2Te_3 ," *Nature Physics* **3**, 1056 (2012).
 - [18] Jin-Peng Xu, Mei-Xiao Wang, Zhi Long Liu, Jian-Feng Ge, Xiaojun Yang, Canhua Liu, Zhu An Xu, Dandan Guan, Chun Lei Gao, Dong Qian, Ying Liu, Qiang-Hua Wang, Fu-Chun Zhang, Qi-Kun Xue, and Jin-Feng Jia, "Experimental detection of a majorana mode in the core of a magnetic vortex inside a topological insulator-superconductor $\text{Bi}_2\text{Te}_3/\text{NbSe}_2$ heterostructure," *Phys. Rev. Lett.* **114**, 017001 (2015).
 - [19] Yan-Feng Lv, Wen-Lin Wang, Yi-Min Zhang, Hao Ding, Wei Li, Lili Wang, Ke He, Can-Li Song, Xu-Cun Ma, and Qi-Kun Xue, "Experimental signature of topological superconductivity and majorana zero modes on $-\text{Bi}_2\text{Pd}$ thin films," *Science Bulletin* **62**, 852 – 856 (2017).
 - [20] Hao-Hua Sun, Kai-Wen Zhang, Lun-Hui Hu, Chuang Li, Guan-Yong Wang, Hai-Yang Ma, Zhu-An Xu, Chun-Lei Gao, Dandan Guan, Yao-Yi Li, Canhua Liu, Dong Qian, Yi Zhou, Liang Fu, Shao-Chun Li, Fu-Chun Zhang, and Jin-Feng Jia, "Majorana zero mode detected with spin selective andreev reflection in the vortex of a topological superconductor," *Phys. Rev. Lett.* **116**, 257003 (2016).
 - [21] Zhijun Wang, P. Zhang, Gang Xu, L. K. Zeng, H. Miao, Xiaoyan Xu, T. Qian, Hongming Weng, P. Richard, A. V. Fedorov, H. Ding, Xi Dai, and Zhong Fang, "Topological nature of the $\text{FeSe}_{0.5}\text{Te}_{0.5}$ superconductor," *Phys. Rev. B* **92**, 115119 (2015).
 - [22] Gang Xu, Biao Lian, Peizhe Tang, Xiao-Liang Qi, and Shou-Cheng Zhang, "Topological superconductivity on the surface of Fe-based superconductors," *Phys. Rev. Lett.* **117**, 047001 (2016).
 - [23] Peng Zhang, Zhijun Wang, Xianxin Wu, Koichiro Yaji, Yukiaki Ishida, Yoshimitsu Kohama, Guangyang Dai, Yue Sun, Cedric Bareille, Kenta Kuroda, *et al.*, "Multiple topological states in iron-based superconductors," *Nature Physics* **15**, 41 (2019).
 - [24] Peng Zhang, Koichiro Yaji, Takahiro Hashimoto, Yuichi Ota, Takeshi Kondo, Kozo Okazaki, Zhijun Wang, Jinsheng Wen, GD Gu, Hong Ding, *et al.*, "Observation of topological superconductivity on the surface of an iron-based superconductor," *Science* **360**, 182–186 (2018).
 - [25] Dongfei Wang, Lingyuan Kong, Peng Fan, Hui Chen, Shiyu Zhu, Wenyao Liu, Lu Cao, Yujie Sun, Shixuan Du, John Schneeloch, *et al.*, "Evidence for majorana bound states in an iron-based superconductor," *Science* **362**, 333–335 (2018).
 - [26] Qin Liu, Chen Chen, Tong Zhang, Rui Peng, Ya-Jun Yan, Chen-Hao-Ping Wen, Xia Lou, Yu-Long Huang, Jin-Peng Tian, Xiao-Li Dong, Guang-Wei Wang, Wei-Cheng Bao, Qiang-Hua Wang, Zhi-Ping Yin, Zhong-Xian Zhao, and Dong-Lai Feng, "Robust and clean majorana zero mode in the vortex core of high-temperature superconductor $(\text{Li}_{0.84}\text{Fe}_{0.16})\text{OHFeSe}$," *Phys. Rev. X* **8**, 041056 (2018).
 - [27] T Machida, Y Sun, S Pyon, S Takeda, Y Kohsaka, T Hanaguri, T Sasagawa, and T Tamegai, "Zero-energy vortex bound state in the superconducting topological surface state of Fe (Se, Te)," *Nature materials* , 1 (2019).
 - [28] C Chen, Q Liu, TZ Zhang, D Li, PP Shen, XL Dong, Z-X Zhao, T Zhang, and DL Feng, "Quantized conductance of majorana zero mode in the vortex of the topological superconductor $(\text{Li}_{0.84}\text{Fe}_{0.16})\text{ohfese}$," *Chinese Physics Letters* **36**, 057403 (2019).
 - [29] Shiyu Zhu, Lingyuan Kong, Lu Cao, Hui Chen, Shixuan Du, Yuqing Xing, Wenyao Liu, Dongfei Wang, Chengmin Shen, and Fazhi Yang, "Observation of Majorana conductance plateau by scanning tunneling spectroscopy," *arXiv e-prints* , arXiv:1904.06124 (2019), arXiv:1904.06124 [cond-mat.supr-con].
 - [30] Lingyuan Kong, Shiyu Zhu, Michał Papaj, Hui Chen, Lu Cao, Hiroki Isobe, Yuqing Xing, Wenyao Liu, Dongfei Wang, Peng

- Fan, *et al.*, “Half-integer level shift of vortex bound states in an iron-based superconductor,” *Nature Physics*, 1–7 (2019).
- [31] Pavan Hosur, Pouyan Ghaemi, Roger S. K. Mong, and Ashvin Vishwanath, “Majorana modes at the ends of superconductor vortices in doped topological insulators,” *Phys. Rev. Lett.* **107**, 097001 (2011).
- [32] Ching-Kai Chiu, Matthew J. Gilbert, and Taylor L. Hughes, “Vortex lines in topological insulator-superconductor heterostructures,” *Phys. Rev. B* **84**, 144507 (2011).
- [33] Hsiang-Hsuan Hung, Pouyan Ghaemi, Taylor L. Hughes, and Matthew J. Gilbert, “Vortex lattices in the superconducting phases of doped topological insulators and heterostructures,” *Phys. Rev. B* **87**, 035401 (2013).
- [34] Shengshan Qin, Lunhui Hu, Xianxin Wu, Xia Dai, Chen Fang, Fu-Chun Zhang, and Jiangping Hu, “Topological vortex phase transitions in iron-based superconductors,” *Science Bulletin* **64**, 1207–1214 (2019).
- [35] Areg Ghazaryan, Pedro L. S. Lopes, Pavan Hosur, Matthew J. Gilbert, and Pouyan Ghaemi, “Effect of Zeeman coupling on the Majorana vortex modes in iron-based topological superconductors,” *arXiv e-prints*, arXiv:1907.02077 (2019), arXiv:1907.02077 [cond-mat.supr-con].
- [36] Sayed Ali Akbar Ghorashi, Taylor L. Hughes, and Enrico Rossi, “Vortex and Surface Phase Transitions in Superconducting Higher-order Topological Insulators,” *arXiv e-prints*, arXiv:1909.10536 (2019), arXiv:1909.10536 [cond-mat.supr-con].
- [37] Xiangang Wan, Ari M. Turner, Ashvin Vishwanath, and Sergey Y. Savrasov, “Topological semimetal and fermi-arc surface states in the electronic structure of pyrochlore iridates,” *Phys. Rev. B* **83**, 205101 (2011).
- [38] Gang Xu, Hongming Weng, Zhijun Wang, Xi Dai, and Zhong Fang, “Chern semimetal and the quantized anomalous hall effect in HgCr_2Se_4 ,” *Phys. Rev. Lett.* **107**, 186806 (2011).
- [39] Zhijun Wang, Yan Sun, Xing-Qiu Chen, Cesare Franchini, Gang Xu, Hongming Weng, Xi Dai, and Zhong Fang, “Dirac semimetal and topological phase transitions in $A_3\text{Bi}$ ($a = \text{Na}, \text{K}, \text{Rb}$),” *Phys. Rev. B* **85**, 195320 (2012).
- [40] S. M. Young, S. Zaheer, J. C. Y. Teo, C. L. Kane, E. J. Mele, and A. M. Rappe, “Dirac semimetal in three dimensions,” *Phys. Rev. Lett.* **108**, 140405 (2012).
- [41] Zhijun Wang, Hongming Weng, Quansheng Wu, Xi Dai, and Zhong Fang, “Three-dimensional dirac semimetal and quantum transport in Cd_3As_2 ,” *Phys. Rev. B* **88**, 125427 (2013).
- [42] Hongming Weng, Chen Fang, Zhong Fang, B. Andrei Bernevig, and Xi Dai, “Weyl semimetal phase in noncentrosymmetric transition-metal monophosphides,” *Phys. Rev. X* **5**, 011029 (2015).
- [43] Shin-Ming Huang, Su-Yang Xu, Ilya Belopolski, Chi-Cheng Lee, Guoqing Chang, BaoKai Wang, Nasser Alidoust, Guang Bian, Madhab Neupane, Chenglong Zhang, *et al.*, “A weyl fermion semimetal with surface fermi arcs in the transition metal monophenictide taas class,” *Nature communications* **6**, 7373 (2015).
- [44] ZK Liu, B Zhou, Y Zhang, ZJ Wang, HM Weng, D Prabhakaran, S-K Mo, ZX Shen, Z Fang, X Dai, *et al.*, “Discovery of a three-dimensional topological dirac semimetal, Na_3Bi ,” *Science* **343**, 864–867 (2014).
- [45] Madhab Neupane, Su-Yang Xu, Raman Sankar, Nasser Alidoust, Guang Bian, Chang Liu, Ilya Belopolski, Tay-Rong Chang, Horng-Tay Jeng, Hsin Lin, *et al.*, “Observation of a three-dimensional topological dirac semimetal phase in high-mobility Cd_3As_2 ,” *Nature communications* **5**, 3786 (2014).
- [46] Sergey Borisenko, Quinn Gibson, Danil Evtushinsky, Volodymyr Zabolotnyy, Bernd Büchner, and Robert J. Cava, “Experimental realization of a three-dimensional dirac semimetal,” *Phys. Rev. Lett.* **113**, 027603 (2014).
- [47] Su-Yang Xu, Ilya Belopolski, Nasser Alidoust, Madhab Neupane, Guang Bian, Chenglong Zhang, Raman Sankar, Guoqing Chang, Zhujun Yuan, Chi-Cheng Lee, Shin-Ming Huang, Hao Zheng, Jie Ma, Daniel S. Sanchez, BaoKai Wang, Arun Bansil, Fangcheng Chou, Pavel P. Shibayev, Hsin Lin, Shuang Jia, and M. Zahid Hasan, “Discovery of a weyl fermion semimetal and topological fermi arcs,” *Science* **349**, 613–617 (2015).
- [48] B. Q. Lv, H. M. Weng, B. B. Fu, X. P. Wang, H. Miao, J. Ma, P. Richard, X. C. Huang, L. X. Zhao, G. F. Chen, Z. Fang, X. Dai, T. Qian, and H. Ding, “Experimental discovery of weyl semimetal taas,” *Phys. Rev. X* **5**, 031013 (2015).
- [49] Ling Lu, Zhiyu Wang, Dexin Ye, Lixin Ran, Liang Fu, John D. Joannopoulos, and Marin Soljačić, “Experimental observation of weyl points,” *Science* **349**, 622–624 (2015).
- [50] N. P. Armitage, E. J. Mele, and Ashvin Vishwanath, “Weyl and dirac semimetals in three-dimensional solids,” *Rev. Mod. Phys.* **90**, 015001 (2018).
- [51] Binghai Yan and Claudia Felser, “Topological materials: Weyl semimetals,” *Annual Review of Condensed Matter Physics* **8**, 337–354 (2017).
- [52] AA Burkov, “Chiral anomaly and transport in weyl metals,” *Journal of Physics: Condensed Matter* **27**, 113201 (2015).
- [53] Shuo Wang, Ben-Chuan Lin, An-Qi Wang, Da-Peng Yu, and Zhi-Min Liao, “Quantum transport in dirac and weyl semimetals: a review,” *Advances in Physics: X* **2**, 518–544 (2017).
- [54] Jin Hu, Su-Yang Xu, Ni Ni, and Zhiqiang Mao, “Transport of topological semimetals,” *Annual Review of Materials Research* **49**, 207–252 (2019).
- [55] Andrew C Potter, Itamar Kimchi, and Ashvin Vishwanath, “Quantum oscillations from surface fermi arcs in weyl and dirac semimetals,” *Nature communications* **5**, 5161 (2014).
- [56] Philip JW Moll, Nityan L Nair, Toni Helm, Andrew C Potter, Itamar Kimchi, Ashvin Vishwanath, and James G Analytis, “Transport evidence for fermi-arc-mediated chirality transfer in the dirac semimetal Cd_3As_2 ,” *Nature* **535**, 266 (2016).
- [57] C. M. Wang, Hai-Peng Sun, Hai-Zhou Lu, and X. C. Xie, “3d quantum hall effect of fermi arcs in topological semimetals,” *Phys. Rev. Lett.* **119**, 136806 (2017).
- [58] Cheng Zhang, Yi Zhang, Xiang Yuan, Shiheng Lu, Jinglei Zhang, Awadhesh Narayan, Yanwen Liu, Huiqin Zhang, Zhuoliang Ni, Ran Liu, *et al.*, “Quantum hall effect based on weyl orbits in Cd_3As_2 ,” *Nature* **565**, 331 (2019).
- [59] Mehdi Kargarian, Mohit Randeria, and Yuan-Ming Lu, “Are the surface fermi arcs in dirac semimetals topologically protected?” *Proceedings of the National Academy of Sciences* **113**, 8648–8652 (2016), <https://www.pnas.org/content/113/31/8648.full.pdf>.
- [60] Alexander Lau, Klaus Koepf, Jeroen van den Brink, and Carmine Ortix, “Generic coexistence of fermi arcs and dirac cones on the surface of time-reversal invariant weyl semimetals,” *Phys. Rev. Lett.* **119**, 076801 (2017).
- [61] Congcong Le, Xianxin Wu, Shengshan Qin, Yinxiang Li, Ronny Thomale, Fu-Chun Zhang, and Jiangping Hu, “Dirac semimetal in -cui without surface fermi arcs,” *Proceedings of the National Academy of Sciences* **115**, 8311–8315 (2018), <https://www.pnas.org/content/115/33/8311.full.pdf>.
- [62] Yun Wu, Na Hyun Jo, Lin-Lin Wang, Connor A. Schmidt, Kathryn M. Neilson, Benjamin Schruck, Przemyslaw Swatek, Andrew Eaton, S. L. Bud’ko, P. C. Canfield, and Adam Kaminski, “Fragility of fermi arcs in dirac semimetals,” *Phys. Rev. B* **99**, 161113 (2019).

- [63] Shengshan Qin, Lunhui Hu, Congcong Le, Jinfeng Zeng, Fuchun Zhang, Chen Fang, and Jiangping Hu, “Quasi-1d topological nodal vortex line phase in doped superconducting 3d dirac semimetals,” *Phys. Rev. Lett.* **123**, 027003 (2019).
- [64] Zhongbo Yan, Fei Song, and Zhong Wang, “Majorana corner modes in a high-temperature platform,” *Phys. Rev. Lett.* **121**, 096803 (2018).
- [65] Supplemental Material.
- [66] Elio J. König and Piers Coleman, “Crystalline-symmetry-protected helical majorana modes in the iron pnictides,” *Phys. Rev. Lett.* **122**, 207001 (2019).
- [67] Andreas P. Schnyder, Shinsei Ryu, Akira Furusaki, and Andreas W. W. Ludwig, “Classification of topological insulators and superconductors in three spatial dimensions,” *Phys. Rev. B* **78**, 195125 (2008).
- [68] Alexei Kitaev, “Periodic table for topological insulators and superconductors,” in *AIP Conference Proceedings*, Vol. 1134 (AIP, 2009) pp. 22–30.
- [69] A Yu Kitaev, “Unpaired majorana fermions in quantum wires,” *Physics-Uspekhi* **44**, 131 (2001).
- [70] M. Wimmer, “Algorithm 923: Efficient numerical computation of the pfaffian for dense and banded skew-symmetric matrices,” *ACM Trans. Math. Softw.* **38**, 30:1–30:17 (2012).
- [71] Alexey A Soluyanov, Dominik Gresch, Zhijun Wang, Quan-Sheng Wu, Matthias Troyer, Xi Dai, and B Andrei Bernevig, “Type-ii weyl semimetals,” *Nature* **527**, 495 (2015).
- [72] Pavan Hosur, Xi Dai, Zhong Fang, and Xiao-Liang Qi, “Time-reversal-invariant topological superconductivity in doped weyl semimetals,” *Phys. Rev. B* **90**, 045130 (2014).
- [73] Shingo Kobayashi and Masatoshi Sato, “Topological superconductivity in dirac semimetals,” *Phys. Rev. Lett.* **115**, 187001 (2015).
- [74] Tatsuki Hashimoto, Shingo Kobayashi, Yukio Tanaka, and Masatoshi Sato, “Superconductivity in doped dirac semimetals,” *Phys. Rev. B* **94**, 014510 (2016).
- [75] Anffany Chen and M. Franz, “Superconducting proximity effect and majorana flat bands at the surface of a weyl semimetal,” *Phys. Rev. B* **93**, 201105 (2016).
- [76] N. P. Butch, P. Syers, K. Kirshenbaum, A. P. Hope, and J. Paglione, “Superconductivity in the topological semimetal YPtBi ,” *Phys. Rev. B* **84**, 220504 (2011).
- [77] Xing-Chen Pan, Xuliang Chen, Huimei Liu, Yanqing Feng, Zhongxia Wei, Yonghui Zhou, Zhenhua Chi, Li Pi, Fei Yen, Fengqi Song, *et al.*, “Pressure-driven dome-shaped superconductivity and electronic structural evolution in tungsten ditelluride,” *Nature communications* **6**, 7805 (2015).
- [78] Defen Kang, Yazhou Zhou, Wei Yi, Chongli Yang, Jing Guo, Youguo Shi, Shan Zhang, Zhe Wang, Chao Zhang, Sheng Jiang, *et al.*, “Superconductivity emerging from a suppressed large magnetoresistant state in tungsten ditelluride,” *Nature communications* **6**, 7804 (2015).
- [79] He Wang, Huichao Wang, Haiwen Liu, Hong Lu, Wuhao Yang, Shuang Jia, Xiong-Jun Liu, XC Xie, Jian Wei, and Jian Wang, “Observation of superconductivity induced by a point contact on 3d dirac semimetal Cd_3As_2 as 2 crystals,” *Nature materials* **15**, 38 (2016).
- [80] Leena Aggarwal, Abhishek Gaurav, Gohil S Thakur, Zeba Haque, Ashok K Ganguli, and Goutam Sheet, “Unconventional superconductivity at mesoscopic point contacts on the 3d dirac semimetal Cd_3As_2 ,” *Nature materials* **15**, 32 (2016).
- [81] He Wang, Huichao Wang, Yuqin Chen, Jiawei Luo, Zhujun Yuan, Jun Liu, Yong Wang, Shuang Jia, Xiong-Jun Liu, Jian Wei, and Jian Wang, “Discovery of tip induced unconventional superconductivity on weyl semimetal,” *Science Bulletin* **62**, 425–430 (2017).
- [82] Maja D. Bachmann, Nityan Nair, Felix Flicker, Roni Ilan, Tobias Meng, Nirmal J. Ghimire, Eric D. Bauer, Filip Ronning, James G. Analytis, and Philip J. W. Moll, “Inducing superconductivity in weyl semimetal microstructures by selective ion sputtering,” *Science Advances* **3** (2017), 10.1126/sciadv.1602983.
- [83] Yanpeng Qi, Pavel G Naumov, Mazhar N Ali, Catherine R Rajamathi, Walter Schnelle, Oleg Barkalov, Michael Hanfland, Shu-Chun Wu, Chandra Shekhar, Yan Sun, *et al.*, “Superconductivity in weyl semimetal candidate MoTe_2 ,” *Nature communications* **7**, 11038 (2016).
- [84] Han-Jin Noh, Jinwon Jeong, En-Jin Cho, Kyoo Kim, B. I. Min, and Byeong-Gyu Park, “Experimental realization of type-ii dirac fermions in a PdTe_2 superconductor,” *Phys. Rev. Lett.* **119**, 016401 (2017).
- [85] H. Leng, C. Paulsen, Y. K. Huang, and A. de Visser, “Type-i superconductivity in the dirac semimetal PdTe_2 ,” *Phys. Rev. B* **96**, 220506 (2017).
- [86] W. Yu, W. Pan, D. L. Medlin, M. A. Rodriguez, S. R. Lee, Zhiqiang Bao, and F. Zhang, “ π and 4π josephson effects mediated by a dirac semimetal,” *Phys. Rev. Lett.* **120**, 177704 (2018).
- [87] An-Qi Wang, Cai-Zhen Li, Chuan Li, Zhi-Min Liao, Alexander Brinkman, and Da-Peng Yu, “ 4π -periodic supercurrent from surface states in Cd_3As_2 nanowire-based josephson junctions,” *Phys. Rev. Lett.* **121**, 237701 (2018).
- [88] Ce Huang, Benjamin T Zhou, Huiqin Zhang, Bingjia Yang, Ran Liu, Hanwen Wang, Yimin Wan, Ke Huang, Zhiming Liao, Enze Zhang, *et al.*, “Proximity-induced surface superconductivity in dirac semimetal Cd_3As_2 ,” *Nature communications* **10**, 2217 (2019).